Nuclear Overhauser Effect Studies of the Conformations of Tetraamminecobalt(III)–Adenosine 5′-Triphosphate Free and Bound to Bovine Heart Protein Kinase†

Paul R. Rosevear, H. Neal Bramson, Catherine O'Brian, E. T. Kaiser, and Albert S. Mildvan*

ABSTRACT: Nuclear Overhauser effects and selective T_1 values were used to determine interproton distances on Co$(NH_3)_4$ATP, free in solution and bound to the catalytic subunit of protein kinase. The distances in free Co$(NH_3)_4$ATP could not be fit by a single conformation and were therefore assumed to result from the averaging of the principal conformations that have been detected by X-ray analysis, and theoretically calculated to be at or near energy minima. Fitting of the interproton distances required the averaging of no fewer than three of these nucleotide conformations. According to these calculations, two anti conformers with glycosidic torsional angles centering at 15° and 55° with extreme C3′-endo and O1′-endo ribose puckers, respectively, contributed approximately 86% to the average structure. A syn conformer with a glycosidic torsional angle centering at 217° and a C2′-endo ribose pucker contributed about 14% to the average structure. The NOE studies thus established the averaging of several conformations of free Co$(NH_3)_4$ATP. Previous paramagnetic probe–T_1 studies of the binary complex of Mn^{2+} and Co$(NH_3)_4$ATP [Granot, J., Kondo, H., Armstrong, R. N., Mildvan, A. S., & Kaiser, E. T. (1979) *Biochemistry 18*, 2339] when interpreted as a root mean sixth average of distances in these three conformers yielded, within experimental error, the measured Mn^{2+}–proton distances. In contrast, the interproton distances on enzyme-bound Co$(NH_3)_4$ATP were fit by a single nucleotide conformation with a high anti glycosidic torsional angle (χ = 78 ± 10°) and an O1′-endo ribose pucker or a mixture of ribose puckers. This conformation of Co$(NH_3)_4$ATP, which is unaltered by saturating the inhibitory site of the enzyme with Mg^{2+}, is indistinguishable from one of two alternative conformations, previously determined by distances from Mn^{2+} at the inhibitory site of the enzyme to the protons and phosphorus nuclei of bound Co$(NH_3)_4$ATP [Granot, J., Kondo, H., Armstrong, R. N., Mildvan, A. S., & Kaiser, E. T. (1979) *Biochemistry 18*, 2339]. The consistency of the conformations of enzyme-bound Co$(NH_3)_4$ATP found by two independent methods with differing reference points and observation frequencies indicates a unique conformation of the bound nucleotide. As protein kinase loses activity with time, the interproton NOE's change in a manner indicating that Co$(NH_3)_4$ATP remains bound to the enzyme. However, the protein structure at the nucleotide binding site alters, allowing the glycosidic conformational angle of Co$(NH_3)_4$ATP to relax to a lower anti value.

Adenosine cyclic 3′,5′-phosphate (cAMP)[1] dependent protein kinase (EC 2.7.1.37; ATP:protein phosphotransferase) is one of a class of enzymes responsible for the regulation of other enzymes or of entire metabolic pathways through selective phosphorylations (Krebs & Beavo, 1979).

Kinetic, structural, and regulatory properties of the bovine heart cAMP-dependent protein kinase have been studied by magnetic resonance methods (Granot et al., 1980). The binding of metal complexes of nucleotide substrates and substrate analogues to the catalytic subunit of protein kinase was shown to induce the appearance of an additional inhibitory divalent cation binding site (Armstrong et al., 1979). The conformation of the enzyme-bound, substitution inert complex β,γ-bidentate Co$(NH_3)_4$ATP was studied by using Mn^{2+} at the inhibitory site as a paramagnetic reference point (Granot et al., 1979a). The Δ-isomer of Co$(NH_3)_4$ATP functions as a slow substrate of protein kinase and competes against MgATP or MnATP for the nucleotide binding site of the enzyme (Granot et al., 1979a,b). Paramagnetic effects of Mn^{2+} on the longitudinal relaxation rates of six carbon-bound protons and the three phosphorus atoms of Co$(NH_3)_4$ATP were used to determine distances from the Mn^{2+} to these nuclei (Granot et al., 1979a). The use of these nine distances in a computer search procedure yielded two sets of solutions for the conformation of enzyme-bound Co$(NH_3)_4$ATP with torsional angles (χ) at the glycosidic bond differing by 200°. One set of solutions showed an anti conformation (χ = 84 ± 10°; Figure 1A,B) while the other showed a syn conformation (χ = 284 ± 10°; Figure 1C,D) (Granot et al., 1979a). From the metal-nuclear distances alone, this ambiguity could not be resolved, nor could the conformation of the ribose ring be evaluated. Moreover, a system that was partially inhibited due to the presence of Mn^{2+} at the inhibitory site had been studied. For these reasons an independent method, the time dependence of the nuclear Overhauser effect (NOE), is used here to reexamine the conformation of the bound nucleotide substrate Co$(NH_3)_4$ATP. For comparison with bound nucleotide, the NOE method is also applied to study the conformation of the free nucleotide.

Our results are consistent with the existence of free Co$(NH_3)_4$ATP as a mixture of syn and anti conformers in so-

† From the Department of Physiological Chemistry, Johns Hopkins University School of Medicine, Baltimore, Maryland 21205 (P.R.R. and A.S.M.), the Laboratory of Bioorganic Chemistry and Biochemistry, Rockefeller University, New York, New York 10021 (H.N.B. and E.T.K.), and the Department of Biochemistry, University of Chicago, Chicago, Illinois 60637 (C.O.B.). *Received January 25, 1983.* This work was supported by National Institutes of Health Grants AM28616 and GM19037, National Science Foundation Grant PCM8121355, and American Cancer Society Postdoctoral Fellowship PF2111 to P.R.R. Support for the computation was provided by National Institutes of Health Grant CA22780. A preliminary report of this work has been published (Rosevear et al., 1981).

[1] Abbreviations: cAMP, adenosine cyclic 3′,5′-phosphate; Co$(NH_3)_4$ATP, tetraammine(adenosine triphosphate-P^β,P^γ)cobalt(III); NOE, nuclear Overhauser effect; DTT, dithiothreitol; A/D, analogue to digital; dGMP, deoxyguanosine 5′-phosphate; DSS, sodium 4,4-dimethyl-4-silapentane-1-sulfonate; PEI, poly(ethylenimine); Tris, tris(hydroxymethyl)aminomethane.

0006-2960/83/0422-3439$01.50/0

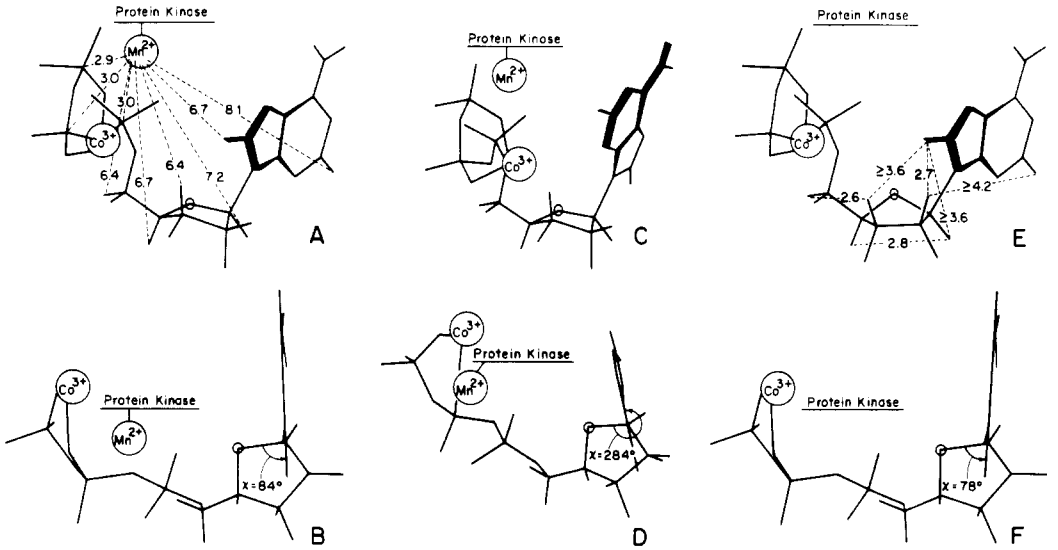

FIGURE 1: Comparison of the conformations of $Co(NH_3)_4ATP$ bound to the catalytic subunit of protein kinase, as determined by the paramagnetic probe–T_1 and NOE methods. Conformations A,B and C,D are alternative fits based on measured distances from Mn^{2+} bound to the inhibitory site (Granot et al., 1979a). Conformation E,F is based on interproton distances determined by NOE and selective T_1 measurements (Tables III and IV).

lution, as has been found for other nucleosides and nucleotides (Schirmer et al., 1970, 1972; Son et al., 1972; Chachaty et al., 1976). For $Co(NH_3)_4ATP$ bound to the catalytic subunit of protein kinase, our data detect a high anti glycosidic torsional angle ($\chi = 78 \pm 10°$) and rule out the syn conformation. Information is also provided on the ribose pucker and on the uniqueness of the conformations of the free and bound nucleotides. The present results thus confirm and extend our previous paramagnetic probe studies (Granot et al., 1979a), by an independent method.

Experimental Procedures

Materials. The catalytic subunit of cAMP-dependent protein kinase from bovine heart muscle was prepared by the method of Demaille et al. (1977), with modifications as previously described (Armstrong et al., 1979; Bramson et al., 1982). The β,γ-bidentate complex of $Co(NH_3)_4ATP$ was prepared as a zwitterion at its isoionic pH as previously described (Cornelius et al., 1977) and characterized by ^{31}P NMR. No impurities were detected by thin-layer chromatography on PEI–cellulose plates developed in 1 M LiCl. Deuterated Tris base was obtained from Stohler. Dowex 50-X2 (100–200 mesh) and Chelex-100 were obtained from Bio-Rad. [γ-^{32}P]ATP was purchased from New England Nuclear. PEI–cellulose plates were purchased from J. T. Baker. All other chemicals were of the highest purity commercially available.

Methods. The concentration of the catalytic subunit was determined spectrophotometrically by using $A^{1\%}_{280} = 14.9$, assuming a molecular weight of 40 000 (Demaille et al., 1977; Armstrong & Kaiser, 1978). The activity of the catalytic subunit was assayed with the synthetic peptide substrate Leu-Arg-Arg-Ala-Ser-Leu-Gly as previously described (Witt & Roskoski, 1975; Armstrong, et al., 1979). Concentrations of $Co(NH_3)_4ATP$ were determined spectrophotometrically by using $\epsilon_{260} = 15.4 \times 10^3\ M^{-1}$. Solutions used in the NMR experiments contained 10 mM deuterated Tris-Cl buffer, pH* 7.5, 150 mM KCl, and 0.1 mM DTT in ^2H_2O. All NMR solutions were passed through Chelex-100 to remove trace metal impurities.

^1H NMR spectra were obtained on a Bruker WM 250 NMR spectrometer by using 16-bit A/D conversion and quadrature phase detection. Chemical shifts were relative to external DSS. The time dependence of the nuclear Overhauser effect was measured by using the following pulse sequence:

$$\{[\text{RD-preirradiate } (t, \omega_1) - \text{observation pulse}]_{16} - [\text{RD-preirradiate } (t, \omega_{\text{off-res}}) - \text{observation pulse}]_{16} - [\text{RD-preirradiate } (t, \omega_2) - \text{observation pulse}]_{16}\}_n$$

where RD is the relaxation delay, t is the duration of preirradiation, and ω_i is the frequency of the irradiated resonance. To ensure complete relaxation between observation pulses, a relaxation delay of $>7T_1$ was used for free $Co(NH_3)_4ATP$ (Canet, 1976) and a relaxation delay $\geq 5T_1$ was used in the presence of protein kinase. A 90° pulse was routinely used for the observation pulse. The pulse sequence was set up in such a way that the free induction decays (FID's) following the irradiation at ω_1, $\omega_{\text{off-res}}$, and ω_2 were each acquired in a separate data block. The FID following irradiation at the control frequency, $\omega_{\text{off-res}}$, was collected either immediately after the FID following irradiation at the observed resonance frequency, ω_1, or immediately prior to ω_2. Irradiations at each of the three frequencies were carried out with the collection of 16 scans in each block. The entire process was repeated 16 times to yield the desired signal/noise in the NOE ($\geq 5/1$).

The proton decoupler was utilized to produce the selective preirradiation pulse of desired duration, t, usually between 0.25 and 2.0 s. Studies on free $Co(NH_3)_4ATP$ in solution typically used a preirradiation pulse power of 20 dB below 0.2 W. The preirradiation pulse used for $Co(NH_3)_4ATP$ bound to the catalytic subunit of protein kinase was typically 32 dB below 0.2 W. These power settings were sufficiently low to selectively irradiate the desired resonances.

The NOE was observed by subtraction of the control FID ($\omega_{\text{off-res}}$) from either of the experimental FID's (ω_1 or ω_2) to yield the appropriate difference FID. The difference FID was Fourier transformed and phased to give negative peaks for negative NOE's and positive peaks for positive NOE's. The magnitude of the NOE was determined either by peak height measurement or by peak integration, which gave indistinguishable results.

The ribose H2′ resonance of $Co(NH_3)_4ATP$ was obscured by the HDO signal and could not be directly observed. In the presence of protein kinase, the chemical shift of the ribose H2′ resonance was therefore always determined by searching for

a frequency which, upon continuous irradiation, decoupled the ribose H1′ resonance.

Longitudinal relaxation rates ($1/T_1$) were measured either by the nonselective saturation–recovery method (Markley et al., 1971) or by a selective method involving the saturation of individual resonances and monitoring their recoveries (Tropp & Redfield, 1981). The pulse sequence used for selective saturation was $[(t,\omega_A)-\tau-$observation pulse–RD$]_n$, where t is the time required for saturation of the resonance A, ω_A is its frequency, τ is the variable delay between the presaturation pulse and the 90° observation pulse, and RD is the relaxation delay to allow magnetic equilibration (>5T_1's). The decoupler was routinely used for the presaturation pulse. For free $Co(NH_3)_4ATP$ in solution, t = 0.15 s at 20 dB below 0.2 W, and for the resonances of $Co(NH_3)_4ATP$ bound to protein kinase, t = 0.1 s at 26 dB below 0.2 W. Transverse relaxation rates ($1/T_2$) were calculated from the line width at half-height ($\Delta\nu$) by using the relation $1/T_2 = \pi\Delta\nu$.

Theory

The nuclear Overhauser effect is defined as a change in the intensity of a nuclear resonance observed upon irradiation of another resonance. NOE's result from the partial transfer of energy from the spin that is being irradiated to neighboring spins, resulting in a change in population of their energy levels. The rate of transfer of energy, or cross-relaxation rate, which is calculated from the NOE, is inversely related to the sixth power of the distance between the irradiated and observed proton and can therefore be used, in favorable cases, to determine interproton distances in the range ≤4 Å (Dubs et al., 1979; Balaram et al., 1972; Tropp & Redfield, 1981). To obtain a better measure of the NOE and to distinguish primary NOE's from secondary and higher order effects, it is best to study the time course of the development of the NOE (Dubs et al., 1979). Primary NOE's are usually observed at early preirradiation times, with secondary effects being observed following a lag period which allows the development of the primary effects.

The magnitude of the final steady-state primary NOE from spin B to spin A will depend on the competition between σ_{AB}, the cross-relaxation rate, or the rate at which energy is transferred from spin B to spin A, and ρ_A, the spin–lattice relaxation rate of spin A. As previously shown (Wagner & Wüthrich, 1979; Dubs et al., 1979), for a two-spin system, the cross-relaxation rate (σ_{AB}) can be calculated from the time dependence of the NOE and the selective longitudinal relaxation rate of spin A (ρ_A) by using eq 1 in which $f_A(B)_t$ is the

$$f_A(B)_t = \frac{\sigma_{AB}}{\rho_A}(1 - e^{-\rho}A^t) + \frac{\sigma_{AB}}{\rho_A - c}(e^{-\rho}A^t - e^{-ct}) \quad (1)$$

NOE to spin A upon preirradiation of spin B for time t, and c is the rate constant for saturation of spin B which is approximated by $^1/_2(1/T_{1B} + 1/T_{2B})$.

In favorable circumstances, the cross-relaxation rate (σ_{AB}) and the correlation function [$f(\tau_r)$] can be used to calculate the distance between nucleus A and nucleus B (r_{AB}) by using

$$r_{AB} = D\left[\frac{f(\tau_r)}{\sigma_{AB}}\right]^{1/6} \quad (2)$$

where the constant D, $(\gamma^4\hbar^2/10)^{1/6}$, is numerically equal to 62.02 Å·s$^{-1/3}$ if A and B are protons and the correlation function $f(\tau_r)$ is given by

$$f(\tau_r) = \frac{6\tau_r}{1 + 4\omega_I^2\tau_r^2} - \tau_r \quad (3)$$

In eq 3 ω_I is the nuclear precession frequency and τ_r is the correlation time. Equations 2 and 3 assume isotropic rotation of the molecule as a whole with a time constant τ_r shorter than any time constants of internal motion (Kalk & Berendsen, 1976). This approximation was justified by the results. The correlation time τ_r was calculated by assuming a fixed distance, independent of conformation, of 2.9 ± 0.2 Å between ribose H1′ and H2′, based on model building (deLeeuw et al., 1980) and crystallographic studies (Lai & Marsh, 1972; Neidle et al., 1976). Its upper limit was estimated with eq 4 (Solomon,

$$\frac{T_1}{T_2} = \frac{12\omega_I^4\tau_r^4 + 37\omega_I^2\tau_r^2 + 10}{16\omega_I^2\tau_r^2 + 10} \quad (4)$$

1955) from the ratios (T_1/T_2) of the longitudinal and transverse relaxation rates of the substrate protons.

Experimentally, NOE's observed on free ligands are easily distinguished from NOE's on bound ligands by two criteria. First, as may be seen from eq 2 and 3, NOE's on a rapidly rotating small ligand result in an enhancement of the observed resonance intensity since $\omega_I\tau_r < 1.12$, while NOE's on an enzyme-bound ligand result in a decrease in the observed resonance intensity since $\omega_I\tau_r > 1.12$. Second, because of the faster relaxation rates of a ligand bound to a macromolecule, the value of c in eq 1 is greater; hence the preirradiation time required to observe an NOE on a ligand bound to a macromolecule is generally less than the preirradiation time required to observe a NOE on a free, rapidly rotating ligand with slower relaxation rates.

Results and Discussion

Interproton Overhauser Effects on Free $Co(NH_3)_4ATP$. The proton NMR spectra of 10 mM $Co(NH_3)_4ATP$ used to evaluate the magnitude of the NOE's were recorded at 250 MHz. The control spectrum (Figure 2A) was obtained by preirradiating the sample for 1 s at 2.43 ppm, a spectral region not containing $Co(NH_3)_4ATP$ resonances. Preirradiation of ribose H2′, at 4.75 ppm for 1 s, gave spectrum B (Figure 2B). NOE's resulting from preirradiation of ribose H2′ are seen in the difference spectrum (Figure 2C) obtained by subtracting the control spectrum A from spectrum B. The difference spectrum (Figure 2C) shows positive primary NOE's from ribose H2′ to adenine H8 and to ribose H1′. Primary NOE's to adenine H8 were also observed from preirradiation of either ribose H1′ or ribose H3′ (spectra not shown). No detectable NOE's to adenine H2 (<0.5%) were observed on preirradiation of any of the proton resonances of $Co(NH_3)_4ATP$. From the time dependence of the primary Overhauser effects and the selective longitudinal relaxation rates, the cross-relaxation rates (σ_{AB}) were calculated by using eq 1 (Table I).

The calculation of distances from the cross-relaxation rates requires a value of the correlation time (τ_r). The τ_r value was estimated by assuming the distance from ribose H1′ to ribose H2′ to be 2.9 Å. Model building studies indicate that this distance lies within the limits of 2.9 ± 0.2 Å regardless of the ribose conformation or the glycosyl torsional angle (χ) (deLeeuw et al., 1980). Distances from ribose H1′ to ribose H2′ determined in the crystallographic structures of adenosine (Lai & Marsh, 1972) and AMP (Neidle et al., 1976) were also found to be in the range 2.9 ± 0.2 Å. By use of this structurally constrained distance in eq 3, an $f(\tau_r)$ value of 4.6 × 10^{-10} s was calculated from the σ_{AB} (0.042 s^{-1}) for ribose H2′ to ribose H1′ (Table I). This $f(\tau_r)$ value yields a τ_r value of 1 × 10^{-10} s which agrees precisely with that previously found for the binary Mn(II)–ATP complex (Sloan & Mildvan, 1976) and with the upper limit value for the binary Mn(II)–Co-

Table I: NOE Data, Relaxation Rates, and Interproton Distances of Free $Co(NH_3)_4ATP$

irradiated resonance of $Co(NH_3)_4ATP$	observed resonance: AdH8 ρ^a (s^{-1})	AdH8 σ^b (s^{-1})	AdH8 r^c (Å)	H1′ ρ^a (s^{-1})	H1′ σ^b (s^{-1})	H1′ r^c (Å)	H3′ ρ^a (s^{-1})	H3′ σ^b (s^{-1})	H3′ r^c (Å)
H1′	0.68	0.033	3.0						
H2′	0.68	0.079	2.6	0.45	0.042	2.9[d]	1.16	0.100	2.5
H3′	0.68	0.025	3.2						
H4′				0.45	0.035	3.0			

[a] The errors in ρ are typically ±10%. [b] The errors in σ are typically ±20%. [c] Distance from irradiated to observed proton calculated by using $f(\tau_r)$ value of 4.55×10^{-10} s from the τ_r value of 1×10^{-10} s. The errors in r are at most ±5%. [d] Assumed, as discussed in the text.

Table II: Conformations Contributing to the Structure of Free $Co(NH_3)_4ATP$ in Solution

conformation[a] name	glycosidic torsional angle (χ) (deg)	ribose pucker	distances[b] (Å): from adenine H8 to ribose H1′	H2′	H3′	from ribose H1′ to H4′	from Mn^{2+} to ribose[c] H1′	H3′	H4′	H5′	fractional population[d]
I	50–60	O1′-endo	3.8	2.4	3.2	2.8	7.9	9.0	9.8	8.8	0.44 ± 0.14
II	44–52	C2′-endo	3.8	2.5	3.8	3.5	7.8	10.1	9.9	8.7	0.07 ± 0.07
III	10–20	C3′-endo	3.7	4.1	3.3	3.2	7.7	8.6	9.8	9.2	0.35 ± 0.11
IV	200–234	C2′-endo	2.3	3.7	5.6	3.5	7.0	8.5	7.8	8.6	0.14 ± 0.05
$\langle r \rangle_{calcd}$[e,f]			3.3	2.6	3.2	3.0	7.6	8.8	9.9	8.9	
$\langle r \rangle_{obsd}$[g,h]			3.3 ± 0.3	2.6 ± 0.3	3.2 ± 0.3	3.0 ± 0.2	8.4 ± 0.6	8.4 ± 0.6	8.6 ± 0.6	7.8 ± 1.0	

[a] Conformations were chosen based on those most frequently found by crystallographic analysis and predicted by theoretical studies to be at or near an energy minimum (deLeeuw et al., 1980; Berthod & Pullman, 1973; Yathindra & Sundaralingam, 1973). [b] Distances (±0.2 Å) determined by model building for the indicated range of glycosidic torsional angles and ribose puckers. [c] Distances within each individual conformation were measured by placing the Mn^{2+} atom 5.4 Å from adenine H8 and 7.2 Å from adenine H2 (Granot et al., 1979a) with the Mn^{2+} atom 3 Å out of the adenine ring plane on the same side of the purine ring as O1′ when the glycosidic torsional angle of $Co(NH_3)_4ATP$ is anti. [d] Fractional populations of the various conformations of $Co(NH_3)_4ATP$ were calculated from simultaneous eq 5–8 by using the theoretical interproton distances in each conformation and the experimentally measured interproton distances as determined by the NOE (Table I). [e] Calculated and observed interproton distances were constrained to be equal by using simultaneous eq 5–8 to calculate the fractional populations. [f] Calculated Mn^{2+}-proton distances are based on the theoretical distances determined by model building of conformations I–IV and on the fractional populations based on the interproton NOE's. [g] Observed interproton distances. See footnote *e*. [h] Observed Mn^{2+}-proton distances were determined by paramagnetic effects on T_1 (Granot et al., 1979a).

$(NH_3)_4ATP$ complex (Granot et al., 1979a), obtained by $1/T_1$ measurements of water protons. The agreement of the τ_r values of the ribose and water protons in these metal–ATP complexes justifies the assumptions used in the derivation of eq 2 and 3 (Kalk & Berendsen, 1976). Internuclear distances calculated from eq 2 using the appropriate cross-relaxation rates and the $f(\tau_r)$ value of 4.6×10^{-10} s are given in Table I.

Conformation of Free $Co(NH_3)_4ATP$. As has been found for other nucleotides in solution (Schirmer et al., 1970; Son et al., 1972; Gueron et al., 1973; Ludemann et al., 1975; Chachaty et al., 1976)[2] the interproton distances of Table I could not be fit by a single conformation of free $Co(NH_3)_4ATP$. This may be shown as follows. The distances from ribose H2′ and ribose H3′ to adenine H8 (Table I)

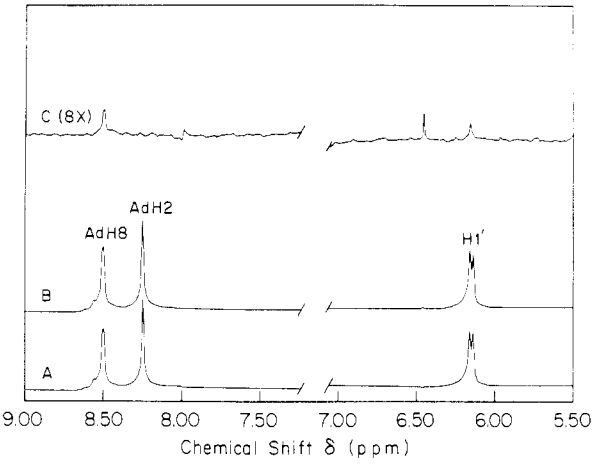

FIGURE 2: Proton NMR spectra of free $Co(NH_3)_4ATP$ used to obtain nuclear Overhauser effects. The sample contained 10 mM $Co(NH_3)_4ATP$, 10 mM deuterated Tris-HCl buffer, 0.15 M KCl, and 0.1 mM DTT at pH* 7.5 in ^2H_2O. (A) The control spectrum with preirradiation at 2.43 ppm for 1 s. (B) Spectrum resulting from preirradiation of ribose H2′ for 1 s. (C) NOE difference spectrum obtained by subtracting the control spectrum A from spectrum B. NMR spectra were obtained with 16-bit A/D conversion, 8192 data points, an acquisition time of 1.64 s, a delay time of 14 s, a spectral width of 2500 Hz, quadrature phase detection, a 90° pulse, and a decoupler power of 20 dB below 0.2 W. T = 25 °C. A total of 64 transients were collected in blocks of 8 transients each. Four scans preceded the collection of each data block to improve cancellation by ensuring a steady state. A line broadening of 2 Hz was used in processing of all data.

[2] A simplified model of nucleotide conformations in solution involving the averaging of two syn and one anti species has been used by Gueron and co-workers to interpret nuclear Overhauser effects (Son et al., 1972; Gueron et al., 1973). NOE's from ribose H1′ to adenine H8 were assumed to reflect syn conformers, while Overhauser effects from ribose H2′ and ribose H3′ to adenine H8 were considered to reflect anti conformers. However, several problems exist with this simplified approach. Distances within the conformers were measured from molecular models neglecting the puckering of the ribose ring. More seriously, the χ angles used to fit the NOE data (70°, 120°, and 300°) were chosen to minimize interproton distances and are therefore near energy maxima rather than energy minima, as predicted from theoretical studies (Berthod & Pullman, 1973; Yathindra & Sundaralingam, 1973) and from model building. Hence these species would not be expected to to contribute significantly to the average nucleotide conformation. Also contrary to the basic assumptions of the simplified theory, model building studies indicate that NOE's from ribose H1′ to adenine H8 may occur in anti conformations ($0° \leq \chi \leq 15°$) and NOE's from ribose H2′ to adenine H8 may occur in syn conformations ($90° \leq \chi \leq 185°$). Ludemann et al. (1975) have also criticized the explicit assumption made by Son et al. (1972) that the Overhauser effect between a ribose proton and adenine H8 is negligible unless the two protons are at their minimal distance.

require a glycosidic torsional angle (χ) in the range 35–45°. Crystallographic studies (Sussman et al., 1972; Rubin et al., 1972; Shikata et al., 1973) and model building (Ludemann et al., 1975) of AMP derivatives having χ angles in this range are found to have distances from ribose H1′ to adenine H8 of 3.9 ± 0.1 Å which are independent of the ribose pucker when χ is held constant. The Overhauser effect from ribose H1′ to adenine H8 yields an average distance of 3.0 ± 0.2 Å between these protons (Table I). This short distance requires the additional contribution of other conformations of $Co(NH_3)_4ATP$ such as syn conformations ($\chi > 90°$) in which this interproton distance is less than 3.0 Å (Table II), as shown by model building (Ludemann et al., 1975) and by crystallographic studies (Rao & Sundaralingam, 1970). Moreover, the short distance of 3.0 Å from ribose H1′ to ribose H4′ determined by the Overhauser effect between these protons (Table I) indicates the contribution of a species with an O1′-endo ribose pucker (Table II). Hence four of the six interproton distances measured on free $Co(NH_3)_4ATP$ (Table I) which are sensitive to conformation require the averaging of several conformers. Two of the measured distances (Table I), those from H2′ to H1′ and from H2′ to H3′, are relatively insensitive to the ribose conformation.

Three species were chosen to contribute to the average [II, III, and IV (Table II)] based on those three conformations of purine nucleosides and nucleotides most frequently found by X-ray (de Leeuw et al., 1980) and predicted by theoretical studies to be at or near an energy minimum (Berthod & Pullman, 1973; Yathindra & Sundaralingam, 1973; Levitt & Warshel, 1978). An additional species [I (Table II)] was chosen with an O1′-endo ribose conformation and an anti glycosidic torsional angle ($\chi = 55 \pm 5°$) in accord with the two known X-ray structures of nucleotides with an O1′-endo ribose pucker (deLeeuw et al., 1980). The interproton distances for each of these four species were calculated from the crystallographic coordinates and from models (Table II). These distances were used together with the four measured conformationally sensitive distances (Table I), in sets of three, in simultaneous equations of the form 5–8 to estimate the

$$\langle r_{AB}^{-6} \rangle = f_I(r_{I,AB})^{-6} + \ldots + f_{IV}(r_{IV,AB})^{-6} \quad (5)$$

$$\langle r_{CD}^{-6} \rangle = f_I(r_{I,CD})^{-6} + \ldots + f_{IV}(r_{IV,CD})^{-6} \quad (6)$$

$$\langle r_{EF}^{-6} \rangle = f_I(r_{I,EF})^{-6} + \ldots + f_{IV}(r_{IV,EF})^{-6} \quad (7)$$

$$\sum f_i = 1.0 \quad (8)$$

fractional contribution of each species. In these equations $\langle r_{AB} \rangle$, $\langle r_{CD} \rangle$, etc., refer to the time averages of the individual interproton distances, and f_i represents the fractional contribution of the ith species to the average. The solution to simultaneous eq 5–8 indicated that one of the four species, a C2′-endo high anti conformation, did not contribute significantly (≤7%) to the average. Solutions of three simultaneous equations omitting conformation II yielded fractional distributions in agreement with those in Table II. The three other species considered (I, III, and IV), anti conformations with O1′-endo and C3′-endo ribose puckers, together with a C2′-endo syn conformation, all contributed significantly to the overall structure of $Co(NH_3)_4ATP$ in solution (Table II). Simpler assumptions involving the averaging of fewer than three species did not yield realistic and self-consistent fits to the measured distances of Table I.[2]

The use of three conformations to fit the four interproton distances measured by NOE methods is supported not only by the internal consistency of the NOE data but also by independent paramagnetic probe–T_1 data on the Mn^{2+} complex of $Co(NH_3)_4ATP$ (Granot et al., 1979a). Thus, using the fractional populations of the four conformers determined from the NOE data (Table II) and placing Mn^{2+} 3 Å out of the adenine ring plane in accord with its measured distances from adenine H2, H8, and the three phosphorus nuclei in each conformer (Granot et al., 1979a) yielded average distances from Mn^{2+} to the ribose protons in agreement with their measured values, and within their experimental errors (Table II). The mobility of the $Co(NH_3)_4$–triphosphate chain renders the distances to phosphorus a less restrictive constraint. From Table II it may be seen that the anti conformers contribute an estimated 86% and the syn conformer 14% to the average structure of $Co(NH_3)_4ATP$ in solution.[3]

Conformation of $Co(NH_3)_4ATP$ Bound to Protein Kinase. Previous measurements of the distances from enzyme-bound Mn^{2+} to the protons and phosphorus atoms of bound $Co(NH_3)_4ATP$ by the paramagnetic probe–T_1 method could not distinguish between a high anti conformation ($\chi = 84 \pm 10°$) (Figure 1A,B) and a syn conformation ($\chi = 284 \pm 10°$) (Figure 1C,D) about the glycosidic bond of the bound nucleotide (Granot et al., 1979a). The nuclear Overhauser effect was used to clarify this point and to evaluate the uniqueness of the conformation of enzyme-bound $Co(NH_3)_4ATP$.

To identify the carbon-bound proton resonances of $Co(NH_3)_4ATP$ unambiguously, the catalytic subunit of protein kinase (0.2 mM) was titrated with $Co(NH_3)_4ATP$, monitoring the proton NMR spectrum. The final concentration of $Co(NH_3)_4ATP$ (2.2 mM) was chosen to be high enough to obtain NOE's with ≥5/1 signal to noise ratio in 30–40 min and low enough to prevent dilution of the NOE by a large pool of free $Co(NH_3)_4ATP$. From the concentrations used, and the dissociation constant of $Co(NH_3)_4ATP$ [$K_D = 301$ μM (Armstrong et al., 1979)], the catalytic subunit of protein kinase was estimated to be 86% saturated with $Co(NH_3)_4ATP$. The initial NOE experiment consisted of a survey of all of the carbon-bound proton resonances of $Co(NH_3)_4ATP$ at a constant preirradiation time (0.5 s). Results from the initial survey were then used to determine at which resonances a complete time dependence of the NOE would be measured.

Typical 250-MHz proton NMR spectra of 2.2 mM $Co(NH_3)_4ATP$ and 0.22 mM catalytic subunit of protein kinase are shown in Figure 3. The control spectrum (Figure 3A) was acquired with a preirradiation time of 0.3 s at 9.53 ppm, a frequency chosen to be distant from $Co(NH_3)_4ATP$ and from protein resonances. Control spectra in which proton resonances of the protein with chemical shifts near those of the ribose and aromatic protons of $Co(NH_3)_4ATP$ were irradiated also yielded no Overhauser effects. Preirradiation of ribose H2′ at 4.77 ppm for 0.3 s (Figure 3B) resulted in small negative NOE's to adenine H8 and to ribose H1′ as observed in the difference spectrum (Figure 3C), obtained by subtracting spectrum A from spectrum B and increasing the gain 16-fold. The time dependences of the Overhauser effects, observed upon preirradiation of ribose H2′ (Figure 4), were used to separate primary from secondary effects. Because of their rapid appearance, Overhauser effects to both adenine H8 and ribose H1′ were judged to be primary (Figure 4). The initial lag in observing the primary NOE's results from the time required to saturate the ribose H2′ resonance, an effect which is approximated by the rate constant c in eq 1. When the resonance of ribose H2′ was preirradiated for longer times (Figure 4), a secondary NOE to adenine H2 was observed. No other

[3] Differences may exist in the conformer distributions of the individual Δ and Λ stereoisomers of free $Co(NH_3)_4ATP$. These distributions are under investigation.

Table III: NOE Data, Relaxation Rates, and Interproton Distances of $Co(NH_3)_4ATP$ Bound to Protein Kinase

irradiated resonance of $Co(NH_3)_4ATP$	observed resonance: AdH8 ρ^a (s^{-1})	AdH8 σ^b (s^{-1})	AdH8 r^c (Å)	H1′ ρ^a (s^{-1})	H1′ σ^b (s^{-1})	H1′ r^c (Å)	H5′ ρ^a (s^{-1})	H5′ σ^b (s^{-1})	H5′ r^c (Å)
H2′	2.78	−0.14	2.7	0.68	−0.10	2.9[d]			
H3′							2.38	−0.19	2.6
H4′				0.68	−0.11	2.8			

[a] The errors in ρ are typically ±5%. [b] The errors in σ are typically ±10%. [c] Calculated by using τ_r value of $(1.4 \pm 0.4) \times 10^{-9}$ s as discussed in the text. The errors in the absolute distances are typically ±10% while those in the relative distances are ±2%. [d] Assumed, as discussed in the text.

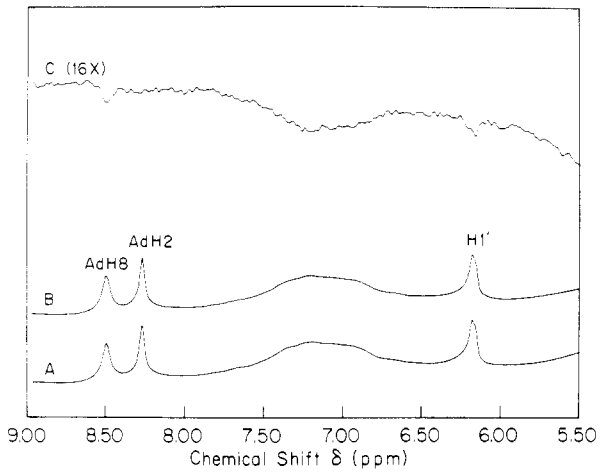

FIGURE 3: Proton NMR spectra of $Co(NH_3)_4ATP$ in the presence of the catalytic subunit of protein kinase, searching for Overhauser effects from ribose H2′. The sample contained 2.2 mM $Co(NH_3)_4ATP$, 0.22 mM catalytic subunit, 10 mM deuterated Tris-HCl buffer, 0.15 M KCl, and 0.1 mM DTT at pH* 7.5 in ^2H_2O. (A) The control spectrum with preirradiation at 9.53 ppm for 0.3 s. (B) Spectrum resulting from preirradiation of ribose H2′ at 4.77 ppm for 0.3 s. (C) NOE difference spectrum obtained by subtracting the control spectrum A from spectrum B. NMR spectra were obtained at 250 MHz with 16-bit A/D conversion by using a total of 256 transients collected in blocks of 16 transients, each of 8192 data points, with an acquisition time of 1.4 s, a delay time of 3.5 s, a spectral width of 3000 Hz, quadrature phase detection, a 90° pulse, and a decoupler power of 26 dB below 0.2 W. T = 25 °C. A line broadening of 2 Hz was used in processing of all data.

NOE's were detected upon preirradiation of ribose H2′, indicating that such effects were less than 1%. Primary NOE's evaluated by the time dependence of the NOE were also observed from ribose H3′ to ribose H5′ and from ribose H4′ to ribose H1′. No other primary NOE's were observed upon preirradiation of any of the carbon-bound protons of $Co(NH_3)_4ATP$.

From the time dependence of the primary NOE's and the longitudinal relaxation rates after selective saturation of the individual resonances, the cross-relaxation rates (σ_{AB}) for the various interproton interactions were calculated by using eq 2 (Table III). A cross-relaxation rate of -0.14 s^{-1} was calculated from ribose H2′ to adenine H8 (Table III). By use of the measured longitudinal relaxation rate of adenine H2, 1.1 s^{-1}, and an upper limit NOE of ±1%, cross-relaxation rates from the various carbon-bound ribose protons to adenine H2 are ≤ -0.011 s^{-1}. From the sixth root of the ratio of the measured cross-relaxation rate from ribose H2′ to adenine H8, and the upper limit cross-relaxation rates from ribose H2′ to adenine H2, it is concluded that ribose H2′ is at least 53% farther from adenine H2 than from adenine H8. Similarly, the absence of a primary Overhauser effect from ribose H1′ to adenine H8 (Figure 5) and the longitudinal relaxation rate of adenine H8 (Table III) can be used to estimate a lower limit

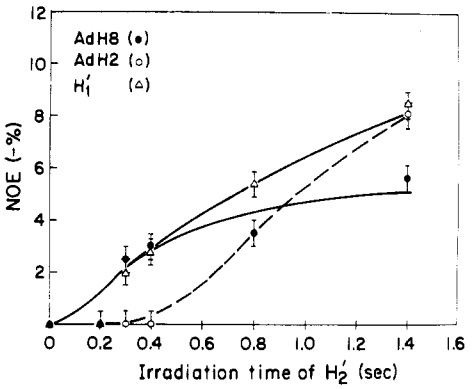

FIGURE 4: Time dependence of the NOE to adenine H8, adenine H2, and ribose H1′ upon preirradiation of ribose H2′. Solid curves represent theoretical fits to the primary effects by using eq 1 where c equals 20 s^{-1} and σ_{AB} is given in Table III. The dashed line represents a secondary NOE from ribose H2′ to adenine H2. Conditions are as given in Figure 3.

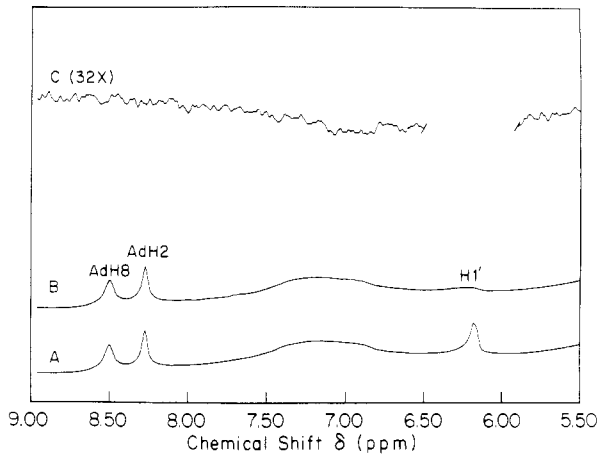

FIGURE 5: Proton NMR spectra of $Co(NH_3)_4ATP$ in the presence of the catalytic subunit of protein kinase, searching for Overhauser effects from ribose H1′. The sample contained 2.2 mM $Co(NH_3)_4ATP$, 0.22 mM catalytic subunit, 10 mM deuterated Tris-HCl buffer, 0.15 M KCl, and 0.1 mM DTT at pH* 7.5 in ^2H_2O. (A) The control spectrum with preirradiation at 9.53 ppm for 0.3 s. (B) Spectrum obtained by preirradiation of ribose H1′ at 6.18 ppm for 0.3 s. (C) NOE difference spectrum obtained by subtracting the control spectrum A from spectrum B. NMR spectra were obtained under the conditions described in Figure 3.

cross-relaxation rate of ≤ -0.028 s^{-1} from ribose H1′ to adenine H8. This indicates that ribose H1′ is at least 31% farther from adenine H8 than from ribose H2′. These relative distances are consistent only with an anti conformation for bound $Co(NH_3)_4ATP$ on the catalytic subunit of protein kinase (Figure 1). From model building, all possible syn conformations of bound $Co(NH_3)_4ATP$ having a primary NOE from ribose H2′ to adenine H8 would also have a primary NOE from ribose H1′ to adenine H8. The latter effect is not observed. The Overhauser effects thus resolve the ambiguity in the confor-

mation of enzyme-bound $Co(NH_3)_4ATP$ determined by the paramagnetic probe–T_1 method (Granot et al., 1979a).

The individual correlation times at 250 MHz for the carbon-bound protons of $Co(NH_3)_4ATP$, estimated from the T_1/T_2 ratio by using eq 4, were averaged to yield a $\tau_r = (2.8 \pm 0.7) \times 10^{-9}$ s for the protein kinase–$Co(NH_3)_4ATP$ complex. Because this τ_r value is an upper limit (Stein & Mildvan, 1978), a more precise value for τ_r is calculated by using the distance from ribose H1′ to ribose H2′ which is structurally constrained to the range 2.9 ± 0.2 Å as determined from X-ray data on nucleosides and nucleotides (Lai & Marsh, 1972; Neidle et al., 1976) and from model building. This distance, together with the σ_{AB} from ribose H2′ to H1′ (Table III), yields from eq 2 and 3 a correlation time (τ_r) of $(1.4 \pm 0.4) \times 10^{-9}$ s. This value of τ_r is consistent with the T_1/T_2 ratio and is within the range $(0.7 \times 10^{-10}$–2.7×10^{-9} s) previously found by the paramagnetic probe–T_1 method in which molecular motion may well contribute to the correlation time (Granot et al., 1979a). The agreement in these τ_r values justifies the assumptions made in deriving eq 2 and 3 (Kalk & Berendsen, 1976). By use of the resulting distances (Table III), model building studies yield a conformation for bound $Co(NH_3)_4ATP$ with a high anti glycosidic torsional angle $\chi = 78 \pm 10°$ (Tables III and IV and Figure 1E,F). This glycosidic torsional angle overlaps with the value of 84 ± 10° on bound $Co(NH_3)_4ATP$ determined independently by the paramagnetic probe–T_1 method (Figure 1A,B) (Granot et al., 1979a). The agreement between these separate measurements of χ based on interproton distances and on Mn^{2+} to proton distances (Granot et al., 1979a) strongly indicates the existence of a unique conformation for bound $Co(NH_3)_4ATP$ on the active catalytic subunit of protein kinase with a high anti glycosidic conformation (Figure 1).

Interproton distances, determined from Overhauser effects, permit only a tentative determination of the ribose conformation on bound $Co(NH_3)_4ATP$ due to an uncertainty of ±10% in the absolute distances and the possibility that the measured NOE's reflect a time average of several ribose conformations. Table IV compares the experimentally determined interproton distances with those derived from models of ATP in which the glycosidic torsional angle is fixed at 78° and ribose is fixed into each of its three extreme conformations, O1′-endo, C2′-endo, or C3′-endo. Included in Table IV is the lower limit distance of ≥3.6 Å from ribose H3′ to adenine H8, based on the absence (<1%) of an observable NOE between these protons. Primary NOE's have previously been observed between ribose H3′ and adenine H8 of MgATP bound to creatine kinase and pyruvate kinase (Rosevear et al., 1981). If a single ribose conformation exists for $Co(NH_3)_4ATP$ on protein kinase, the comparison in Table IV indicates that O1′-endo provides the best fit to the distances. Moreover, the distances rule out a pure C2′-endo or pure C3′-endo sugar pucker. An interconverting mixture of C2′-endo and C3′-endo ribose provides a less satisfactory fit to the measured distances than does a pure O1′-endo ribose conformation (Table IV). However, such a mixture cannot be strictly excluded, nor can a mixture of all three ribose conformations, because of the errors in the measured distances.

It has been shown from X-ray data that C2′-endo ribose conformations tend to accompany high anti glycosidic torsional angles, but this correlation is not absolute (Sundaralingam, 1969; deLeeuw et al., 1980). Thus dGMP has an O1′-endo sugar pucker and a glycosidic torsional angle (χ) of 54° (Young et al., 1974), and theoretical calculations indicate O1′-endo is only slightly higher in energy, by 0.5 kcal/mol, than C2′-endo or C3′-endo (Levitt & Warshel, 1978). One of the two structures of NaATP found crystallographically has a C2′-endo ribose with $\chi = 39°$, and the other has a C3′-endo ribose with $\chi = 69°$ (Kennard et al., 1971). Previous model building studies using distances from Mn^{2+} bound at the inhibitory site of protein kinase to the protons and phosphorus nuclei of bound $Co(NH_3)_4ATP$ (Granot et al., 1979a) had arbitrarily assumed a C3′-endo ribose conformation based on one of the two structures of NaATP found crystallographically. From the present data, this assumption is no longer tenable for $Co(NH_3)_4ATP$ bound to protein kinase.

Table IV: Internuclear Distances Determined from Overhauser Effects and from Model Building of $Co(NH_3)_4ATP$

from	to	measured distance[a] (Å)	distances calculated from model building[b] O1′-endo	C2′-endo	C3′-endo
H1′	H2′	2.9	2.9[c]	2.9[d]	2.9[d]
H1′	H3′		4.0[e]	3.8[d]	3.8[d]
H1′	H4′	2.8	2.8[e]	3.5[d]	3.2[d]
H1′	H5′		4.7	4.9	5.0
H1′	AdH8	≥3.6	4.0[c]	4.0[d]	4.0[d]
H2′	H3′		2.3	2.4[d]	2.4[d]
H2′	H4′		4.0	4.2[d]	3.8[d]
H2′	H5′		4.5	3.8	4.8
H2′	AdH8	2.7	2.7	2.3	3.5[c]
H2′	AdH2	≥4.2	7.2	6.9	6.9
H3′	H4′		3.0	2.8	2.7[d]
H3′	H5′	2.6	2.7	2.7	2.7
H3′	AdH8	≥3.6	3.6	3.9[c]	2.4[c]
H4′	H5′		3.2	3.2	2.9
H4′	AdH8		4.3	4.0[c]	3.9[c]
H5′	AdH8		4.0	4.1	3.3[c]

[a] Measured distances were calculated by using a $\tau_r = 1.4 \times 10^{-9}$ s in eq 2 and 3 as discussed in the text. [b] Distances on $Co(NH_3)_4ATP$ were calculated from framework molecular models by using a glycosidic torsional angle of 78°. Errors in the distances obtained from model building are ±0.2 Å, except for distances involving ribose H5′, which are accurate to ±0.3 Å. Interproton distances to ribose H5′ and H5″ were measured as the average distance to each by using the Mn^{2+} to ^{31}P NMR distances of Granot et al. (1979a) to fix the position of the α phosphorus of $Co(NH_3)_4ATP$ with respect to adenosine. [c] Measured distances in agreement with those obtained by model building studies of Ludemann et al. (1975). [d] Measured distances in agreement with those calculated from models by deLeeuw et al. (1980). [e] Measured distances in agreement with the crystal structure of 1-β-D-arabinofuranosylthymine, found to have an O1′-endo ribose sugar conformation (Tougard, 1973).

Effect of Mg^{2+} at the Inhibitory Site on the Conformation of Enzyme-Bound $Co(NH_3)_4ATP$. To determine whether a divalent cation at the inhibitory site of protein kinase influences the conformation of bound $Co(NH_3)_4ATP$, interproton NOE's were measured on 1.64 mM $Co(NH_3)_4ATP$ in the presence of 0.21 mM catalytic subunit and 12 mM $MgCl_2$. From the dissociation constant of Mg^{2+} from the inhibitory site of protein kinase [2.3 mM (Armstrong et al., 1979)] this site was 84% occupied by Mg^{2+} under these conditions. A preirradiation time of 0.3 s was used to avoid the complications of secondary Overhauser effects and spin diffusion. A primary NOE was observed from ribose H2′ to adenine H8, of the same magnitude as had been observed in the absence of Mg^{2+}. No Overhauser effects were observed from ribose H1′ and ribose H3′ to adenine H8 or from either ribose H2′ or ribose H3′ to adenine H2. These results, which are indistinguishable from those observed in the absence of Mg^{2+}, show that the observed conformation of bound $Co(NH_3)_4ATP$ is unaffected by binding of the inhibitory divalent cation; i.e., $Co(NH_3)_4ATP$ retains its high anti glycosidic torsional angle with either an O1′-endo or a mixture of ribose conformations (Table IV).

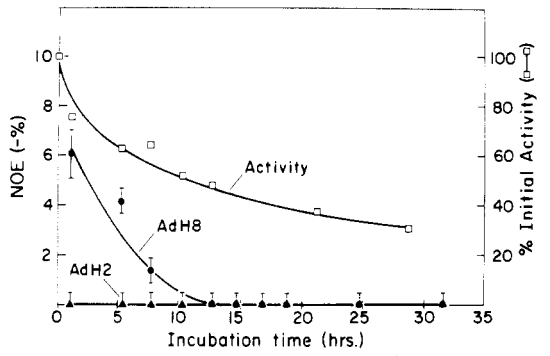

FIGURE 6: Time dependence of the catalytic activity of protein kinase and the magnitude of the ribose H2′ to adenine H8 primary NOE during incubation of the enzyme in the NMR spectrometer. $T = 25$ °C. Conditions for obtaining the NMR spectra are as described in Figure 3. Aliquots (10 μL) were removed and assayed for activity as described under Methods.

A change in the glycosidic torsional angle of bound Co$(NH_3)_4$ATP upon the addition of Mg^{2+} at the inhibitory site would not have been expected since the inhibitory metal is known to coordinate only the enzyme and the triphosphate chain of bound Co$(NH_3)_4$ATP (Granot et al., 1979a).

Effect of Time-Dependent Inactivation of Protein Kinase on the Conformation of Bound Co$(NH_3)_4$ATP. After prolonged incubation (~30 h) of protein kinase in the NMR spectrometer at 25 °C, it was observed that the primary NOE from ribose H2′ to adenine H8 decreased by a factor of at least 3 to an undetectable level (Figure 6) and the enzymatic activity of protein kinase was diminished by ~70%. A study monitoring the time-dependent loss of catalytic activity and the magnitude of the NOE from ribose H2′ to adenine H8 showed that the loss of enzymatic activity correlated with the loss of the primary NOE between ribose H2′ and adenine H8 (Figure 6 and Table V). This was not due to the dissociation of ATP from the enzyme since the primary Overhauser effects from ribose H2′ to ribose H1′ and from ribose H4′ to ribose H1′ remained negative and constant as the catalytic subunit lost activity (Table V). Moreover, the short preirradiation times required to detect both primary and secondary NOE's with the inactive enzyme are consistent with the short T_1 and T_2 values expected for bound Co$(NH_3)_4$ATP.

The changing patterns of primary and secondary Overhauser effects observed as the enzyme loses activity (Table V) suggest a change in the conformation of bound Co$(NH_3)_4$ATP from a high anti ($\chi = 78 \pm 10°$) to a lower anti glycosidic torsional angle ($\chi \sim 30°$), although more complicated interpretations cannot be excluded. During the loss of enzymatic activity, no new primary NOE's appeared. From the absence of primary Overhauser effects to adenine H8 (<1%) on the inactive enzyme, lower limit distances of ≥3.4 Å can be estimated from ribose H2′ and ribose H3′ to adenine H8 of bound Co$(NH_3)_4$ATP. Model building studies indicate that a nucleotide conformation with a low anti glycosidic torsional angle of approximately 30° would place ribose H2′ and H3′ ≥3.4 Å from adenine H8. The loss of the secondary NOE from ribose H3′ to adenine H8 and the appearance of a secondary NOE from ribose H5′ to adenine H8 as the enzyme loses activity (Table V) suggest a rotation of adenine away from H3′ and toward H5′ as would occur in a low anti conformation. The possibility of a syn conformation at the glycosidic bond of Co$(NH_3)_4$ATP bound on the inactive enzyme can be eliminated by the absence of a primary NOE between ribose H1′ and adenine H8. Model building studies predict such a primary NOE for all glycosidic torsional angles giving a syn conformation.

Table V: Changes in Primary and Secondary Nuclear Overhauser Effects Correlated with Loss of Enzymatic Activity of Protein Kinase[a,b]

irradiated resonance	observed resonance	type of effect	−% NOE[c] active protein kinase	−% NOE[d] inactive protein kinase
H2′	AdH8	primary	6	≤1
H2′	H1′	primary	4	4
H4′	H1′	primary	4	4
H2′	AdH2	secondary	8	10
H3′	AdH8	secondary	5	≤1
H3′	AdH2	secondary	3	4
H4′	AdH8	secondary	≤2	≤2
H4′	AdH2	secondary	≤2	6
H5′	AdH8	secondary	≤2	5
H5′	AdH2	secondary	6	4

[a] Primary NOE's were measured at preirradiation times of either 0.3 or 0.4 s with typical errors of ±1%. [b] Secondary NOE's were measured at preirradiation times of 1.0 s with typical errors of ±2%. [c] Activity of the catalytic subunit of protein kinase was ≥80% of its maximal value. [d] Activity of the inactive catalytic subunit of protein kinase was ≤30% of its maximal value.

The change in the conformation of enzyme-bound Co$(NH_3)_4$ATP which accompanies the loss of activity probably reflects a change in the protein conformation. In accord with this view, a secondary Overhauser effect from ribose H4′ to adenine H2 was observed when the enzyme lost activity (Table V). Due to the large distance (≥5.3 Å) between ribose H4′ and adenine H2 in all conformations of Co$(NH_3)_4$ATP, this secondary effect is most likely transmitted through the protein and requires at least one change in protein structure as the enzyme loses activity.

In conclusion, an analysis of interproton nuclear Overhauser effects indicates that the structure of free Co$(NH_3)_4$ATP in solution is best fit by an average of three conformations, two anti and one syn. The anti conformers have glycosidic torsional angles ranging from 10 to 60°. These results are also consistent with distances from Mn^{2+} to the protons and phosphorus nuclei in the binary Mn^{2+} complex of Co$(NH_3)_4$ATP (Table II; Granot et al., 1979a).

In contrast, the NOE data on Co$(NH_3)_4$ATP bound to the active site of protein kinase are fit by a single conformation with a high anti glycosidic torsional angle ($\chi = 78 \pm 10°$). The Overhauser effects also suggest either an O1′-endo or a mixture of ribose conformations for bound Co$(NH_3)_4$ATP, conclusions which are consistent with earlier paramagnetic probe–T_1 data (Granot et al., 1979a). The mutual consistency of the conformations of enzyme-bound Co$(NH_3)_4$ATP determined by both NOE and the paramagnetic probe–T_1 measurements (Granot et al., 1979a), methods with differing reference points and averaging times, supports the existence of a unique conformation for Co$(NH_3)_4$ATP on protein kinase.

The loss of enzymatic activity of the catalytic subunit of protein kinase was shown to be coincident with the loss of the primary NOE from ribose H2′ to adenine H8 and with changes in secondary NOE's consistent with a perturbation of the enzyme structure at the ATP binding site, which alters the glycosidic conformational angle to a lower anti value. This structural change of bound Co$(NH_3)_4$ATP which accompanies the loss of enzymatic activity may be a part of the inactivation process. Jencks (1975) has suggested that interaction energy at a portion of the substrate binding site remote from the reaction center may be used to drive an enzymatic reaction by distorting the structure of the substrate toward that of the transition state. Although other possibilities exist, one might

speculate that the correlation between the loss of catalytic activity of protein kinase and the change in the glycosidic torsional angle of bound $Co(NH_3)_4ATP$ may represent an example of this effect.

Registry No. $Co(NH_3)_4ATP$, 63915-26-4; protein kinase, 9026-43-1; Mg, 7439-95-4.

References

Armstrong, R. N., & Kaiser, E. T. (1978) *Biochemistry 17*, 2840.

Armstrong, R. N., Kondo, H., Granot, J., Kaiser, E. T., & Mildvan, A. S. (1979) *Biochemistry 18*, 1230.

Balaram, P., Bothner-By, A. A., & Breslow, E. (1972) *J. Am. Chem. Soc. 94*, 4017.

Berthod, H., & Pullman, B. (1973) *FEBS Lett. 33*, 147.

Bramson, H. N., Thomas, N., Matsueda, R., Nelson, N. C., Taylor, S. S., & Kaiser, E. T. (1982) *J. Biol. Chem. 257*, 10575.

Canet, D. (1976) *J. Magn. Reson. 23*, 361.

Chachaty, L., Zemb, T., Langlet, G., & Son, T. (1976) *Eur. J. Biochem. 62*, 45.

Cornelius, R. D., Hart, P. A., & Cleland, W. W. (1977) *Inorg. Chem. 16*, 2799.

deLeeuw, H. P. M., Haasnoot, C. A. G., & Altona, C. (1980) *Isr. J. Chem. 20*, 108.

Demaille, J. G., Peters, K. A., & Fischer, E. H. (1977) *Biochemistry 16*, 3080.

Dubs, A., Wagner, G., & Wuthrich, K. (1979) *Biochim. Biophys. Acta 577*, 177.

Granot, J., Kondo, H., Armstrong, R. N., Mildvan, A. S., & Kaiser, E. T. (1979a) *Biochemistry 18*, 2339.

Granot, J., Mildvan, A. S., Brown, E., Kondo, H., Bramson, H. N., & Kaiser, E. T. (1979b) *FEBS Lett. 103*, 265.

Granot, J., Mildvan, A. S., & Kaiser, E. T. (1980) *Arch. Biochem. Biophys. 205*, 1.

Gueron, M., Chachaty, L., & Son, T. D. (1973) *Ann. N.Y. Acad. Sci. 222*, 307.

Jencks (1975) *Adv. Enzymol. Relat. Areas Mol. Biol. 43*, 219.

Kalk, A., & Berendsen, H. J. C. (1976) *J. Magn. Reson. 24*, 343.

Kennard, O., Isaacs, N. W., Motherwell, W. D. S., Coppola, J. C., Wampler, D. L., Larson, A. L., & Watson, D. G. (1971) *Proc. R. Soc. London, Ser. A 325*, 401.

Krebs, E. G., & Beavo, J. A. (1979) *Annu. Rev. Biochem. 48*, 923.

Lai, T. F., & Marsh, R. E. (1972) *Acta Crystallogr., Sect. B B28*, 1982.

Levitt, M., & Warshel, A. (1978) *J. Am. Chem. Soc. 100*, 2607.

Ludemann, H. D., Roder, O., Westhof, E., Goldammer, E. V., & Muller, A. (1975) *Biophys. Struct. Mech. 1*, 121.

Markley, J. L., Horsley, W. J., & Klein, M. P. (1971) *J. Chem. Phys. 55*, 3604.

Neidle, S., Kuhlbrandt, W., & Achari, A. (1976) *Acta Crystallogr., Sect. B B32*, 1850.

Rao, S. T., & Sundaralingam, M. (1970) *J. Am. Chem. Soc. 92*, 4963.

Rosevear, P. R., Desmeules, P., Kenyon, G. L., Bramson, H. N., Kaiser, E. T., & Mildvan, A. S. (1981) Abstracts of the American Chemical Society Division of Biological Chemistry Meeting, Aug 31–Sept 3, 1981, Abstr. 20.

Rubin, J., Brennan, T., & Sundaralingam, M. (1972) *Biochemistry 11*, 3112.

Schirmer, R. E., Noggle, J. H., Davis, J. P., & Hart, P. A. (1970) *J. Am. Chem. Soc. 92*, 3266.

Schirmer, R. E., Davis, J. P., Noggle, J. H., & Hart, P. A. (1972) *J. Am. Chem. Soc. 94*, 2561.

Shikata, K., Ueki, T., & Mitsui, T. (1973) *Acta Crystallogr., Sect. B B29*, 31.

Sloan, D. L., & Mildvan, A. S. (1976) *J. Biol. Chem. 251*, 2412.

Solomon, I. (1955) *Phys. Rev. 99*, 559.

Son, T. D., Guschlbauer, W., & Gueron, M. (1972) *J. Am. Chem. Soc. 94*, 7903.

Stein, P. J., & Mildvan, A. S. (1978) *Biochemistry 17*, 2675.

Sundaralingam, M. (1969) *Biopolymers 7*, 821.

Sussman, J. L., Seeman, N. C., Kim, S. H., & Berman, H. M. (1972) *J. Mol. Biol. 66*, 403.

Tougard, P. (1973) *Acta Crystallogr., Sect. B B29*, 2227.

Tropp, J., & Redfield, A. G. (1981) *Biochemistry 20*, 2133.

Wagner, G., & Wüthrich, K. (1979) *J. Magn. Reson. 33*, 675.

Witt, J. J., & Roskoski, R., Jr. (1975) *Anal. Biochem. 66*, 253.

Yathindra, N., & Sundaralingam, M. (1973) *Biopolymers 12*, 297.

Young, D. W., Tollin, P., & Wilson, H. R. (1974) *Acta Crystallogr., Sect. B B30*, 2012.